Bull. Mater. Sci. (2018) 41:61
https://doi.org/10.1007/s12034-018-1552-z

A facile approach for the synthesis of porous $KTiNbO_5$ catalyst with good activity for hydrogenation of p-nitrophenol

PING YANG*, JUN HU, YOUCHUN YU and BIN WANG
School of Chemical Engineering, Anhui University of Science and Technology, Huainan, Anhui 232001, People's Republic of China
*Author for correspondence (pyang8066@163.com)

MS received 6 April 2017; accepted 1 July 2017; published online 6 April 2018

Abstract. Through simple ions exchange and hydrothermal reaction, the porous structure of MnO_2-pillared $KTiNbO_5$ composites were synthesized. The fabricated porous structure makes $KTiNbO_5$ as good absorbance property for methylthionine chloride (MB). Furthermore, the as-synthesized porous $KTiNbO_5$ can perform photocatalytic degradation of MB with good effectivity. What's more, after loading Au nanoparticles into it, a novel catalyst for catalytic hydrogenation of p-nitrophenol was obtained. The possible 'layer-by-layer quilt expose' mode of Au-MnO_2-$KTiNbO_5$ composites for catalytic hydrogenation of p-nitrophenol was proposed.

Keywords. Porous structure; MnO_2-pillared $KTiNbO_5$; photocatalytic degradation; catalytic hydrogenation.

1. Introduction

Preparation of p-aminophenol is important in various applications in the chemical industry, biomedicine and colouration [1–3]. This intermediate material is mainly produced by reducing nitrophenol into p-aminophenol [4–6]. Different kinds of catalysts were widely exploited for the hydrogenation of nitrophenol to improve the production of p-aminophenol from the reduction of p-nitrophenol. Currently, some metal or metal oxide-based nanocomposites are widely applied in the hydrogenation of nitrophenol [7–9]. However, extreme reaction or low yield associated with using this catalyst remains a challenge. Improving the availability of the catalyst in the reduction of p-nitrophenol under mild conditions has gained increased attention.

Metallic nanosheets are efficient when used as catalysts to prepare organic compounds [10]. Utilizing metal nanosheet-based catalysts in redox reactions has received increased attention because of two reasons. First, large surface areas of nanosheets prevent loading particles from aggregation, which results in the exposure of sufficient active sites of catalyst to the reactant. Second, no surfactants were used in the process of synthesis of nanosheet-based composites, which improve the catalytic activity better. Among the metal nanosheets, the layered transition metal oxide, $HTiNbO_5$, is widely used as a catalyst in organic reactions with good activity [11,12]. However, the exfoliation of bulk $KTiNbO_5$ into single nanosheets is tedious according to the reported method [13–15]. After stacking the single nanosheets of $HTiNbO_5$ for the construction of 3D materials, a disordered solid structure is produced, which can negatively affect the catalytic activity [16]. Thus, a facile method for constructing metal nanosheet-based catalyst with a unique structure must be developed for organic reactions.

In this study, we synthesized oxide manganese-pillared $KTiNbO_5$ layered composites through facile-ion exchange and a hydrothermal method, which overcame the complicated exfoliation and stacking process. The porous structure was produced as a result of the pillaring action of oxide manganese on the plates of $KTiNbO_5$, resulting in good adsorption to the reactants. After reducing Au ions into Au nanoparticles in the porous $KTiNbO_5$ composites under UV light irradiation, the composites loaded with Au nanoparticles were applied to hydrogenate p-nitrophenol. Interestingly, the as-prepared composites showed better-quality catalytic activity and recyclability after re-using for the third time. Thus, a type of $KTiNbO_5$-based composites with porous structure was synthesized using a facile method and applied in the hydrogenation of p-nitrophenol through a possible 'layer-by-layer quilt exposure' mode.

Electronic supplementary material: The online version of this article (https://doi.org/10.1007/s12034-018-1552-z) contains supplementary material, which is available to authorized users.

2. Experimental

2.1 *Chemicals and materials*

All reagents were of analytical grade and used as received without further purified. Nb_2O_5, K_2CO_3 and TiO_2 (Guoyao Chemical Co., Shanghai, China) were mixed to synthesize layered $KTiNbO_5$. $Mn(NO_3)_2$ (50 wt% in water), SDBS and $KMnO_4$ (Guoyao Chemical Co., Shanghai, China) were purchased to prepare porous $KTiNbO_5$ composites. $HAuCl_4$ (Guoyao Chemical Co., Shanghai, China) was used to synthesize Au nanoparticles in porous $KTiNbO_5$. Methylene blue (MB) (Guoyao Chemicals Co., Shanghai, China) and p-nitrophenol (Guoyao Chemicals Co., Shanghai, China) were applied to evaluate the catalytic properties of the as-synthesized $KTiNbO_5$-based composites.

2.2 *Preparation of porous $KTiNbO_5$ composites*

$KTiNbO_5$ was synthesized through the high-temperature solid state method which was reported by us previously [17]. The ion exchange process was exploited as follows: after dispersing 1 g of $KTiNbO_5$ into 100 ml of 1.5 mol l^{-1} $Mn(NO_3)_2$ aqueous solution, and the mixture is stirred for 24 h at 45°C. Then, the product was collected and dispersed them into the fresh 100 ml of 1.5 mol l^{-1} $Mn(NO_3)_2$ aqueous solution again and repeated the ions exchange process until the supernatant became red. The final products of $K_{1-2x}Mn_xTiNbO_5$ was collected through filtration and washed with deionized water and ethanol for several times.

One gram of $K_{1-2x}Mn_xTiNbO_5$ powder, 0.042 g SDBS and 0.485 g $KMnO_4$ was mixed into the 20 ml deionized water. After stirring for 30 min, the mixture was transferred into the Teflon-lined autoclave reaction for 12 h at 160°C. The as-synthesized porous $KTiNbO_5$ composite was collected and washed with deionized water and ethanol for several times to remove the unreacted impurities.

2.3 *Loading Au nanoparticles into the porous $KTiNbO_5$ composites*

One gram of the as-synthesized porous composites with 6 ml of $HAuCl_4$ (1 wt%) was mixed in 50 ml deionized water. After 2 h stirring, the sediment was collected through natural sedimentation. The Au nanoparticles-loaded porous composites were obtained through irradiation of the sediment with a 500 W mercury lamp for 30 min.

2.4 *Adsorption effect of the as-synthesized porous $KTiNbO_5$ composites on MB*

0.7 millilitres of the as-synthesized porous $KTiNbO_5$ (0.25 g ml^{-1}) composites were mixed with different concentrations of 100 ml (10, 20 and 30 mg l^{-1}) MB. The MB solution was collected by centrifugation every 5 min and measured with a UV–visible spectrophotometer, respectively.

2.5 *Photocatalytic degradation of MB with the as-synthesized porous $KTiNbO_5$*

The process of photocatalytic degradation of MB with the as-synthesized porous $KTiNbO_5$ similar to the adsorption process as described above except a 500 W mercury lamp was used for UV light irradiation. The process to measure the adsorption spectrum of MB is also same to the description above.

2.6 *Catalytic reduction of p-nitrophenol into p-aminophenol with as-synthesized porous $KTiNbO_5$ or Au nanoparticles-loaded porous $KTiNbO_5$ composites*

According to the method reported by us previously [6], the catalytic ability of the Au nanoparticles-loaded porous $KTiNbO_5$ composites or pure porous $KTiNbO_5$ were measured through catalytic reduction of p-nitrophenol. Generally, after mixing the fresh prepared 0.528 mol l^{-1} sodium borohydride (30 ml) and 5.0 mmol l^{-1} p-nitrophenol (20 ml) in a beaker at 45°C for 10 min and 1 ml (0.25 g ml^{-1}) of as-prepared porous $KTiNbO_5$ or Au-loaded porous $KTiNbO_5$ composites were added into the beaker. The supernatant was collected every 5 min through centrifugation. The UV spectrum of the supernatant was measured after diluting them for 5 times, respectively.

2.7 *Characterization of the as-synthesized porous composites*

The inductively coupled plasma emission spectrometer (ICP, SCIEX ELAN DRC-e) was used to analyse the elemental composition. Thermogravimetry analysis (TG; TGA/DSC1, Mettler, Switzerland) was carried out to follow the decomposition of porous $KTiNbO_5$ or Au-loaded porous $KTiNbO_5$ composites with a heating rate of 5°C min^{-1} in the N_2 atmosphere from 30 to 700°C. The UV–visible spectra were studied with a Shimadzu UV-2550 spectrophotometer. The X-ray powder diffraction (PXRD) patterns of the as-synthesized porous $KTiNbO_5$ composites were measured by a Japanese RigakuDmax-GA rotation anode X-ray diffractometer (XRD) equipped with graphite monochromatized CuK α radiation. A Bruker Vector-22 FTIR spectrometer was used to measure the FTIR spectra from 4000 to 400 cm^{-1} at room temperature.

3. Result and discussion

3.1 *Synthesis and characterization of the as-synthesized composites*

Scheme 1 shows the process for the synthesis of porous $KTiNbO_5$ composites loaded with Au nanoparticles. First, $Mn(NO_3)_2$ solution was mixed with the layered $KTiNbO_5$ which was synthesized using a high-temperature solid-phase method [17] (figure 1a) under strong stirring conditions.

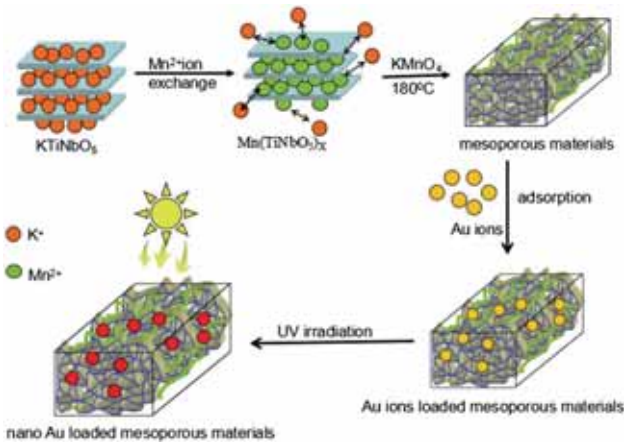

Scheme 1. Fabrication of composites of porous $KTiNbO_5$ loaded with Au nanoparticles.

The ions exchange procedure was repeated for four times, so that all Mn^{2+} ions can exchange with K^+ entirely. The content of manganese in the composites was measured with ICP and the x could be calculated as 0.33 for $K_{1-2x}Mn_x$ $TiNbO_5$. Second, after cleaning the product with ethanol and water several times to remove impurities, manganese ion-exchanged $KTiNbO_5$ was transferred into a Teflon-lined autoclave with $KMnO_4$ and reacted for 24 h at 180°C. The formed oxide manganese nanoparticles in the interlayer of $KTiNbO_5$ pillared the plates and thus, increased the interlayer space of $KTiNbO_5$. Figure 1b shows that the porous structure can be clearly observed. Finally, Au nanoparticles were loaded into oxide manganese nanoparticle-pillared $KTiNbO_5$ under UV light irradiation. However, these findings were not observed in the scanning electron microscopy (SEM) image (figure 1c) possibly because of the small sized Au particles distributed in the pores of the material. The XRD pattern of the as-synthesized porous composites was investigated. Supplementary figure S1

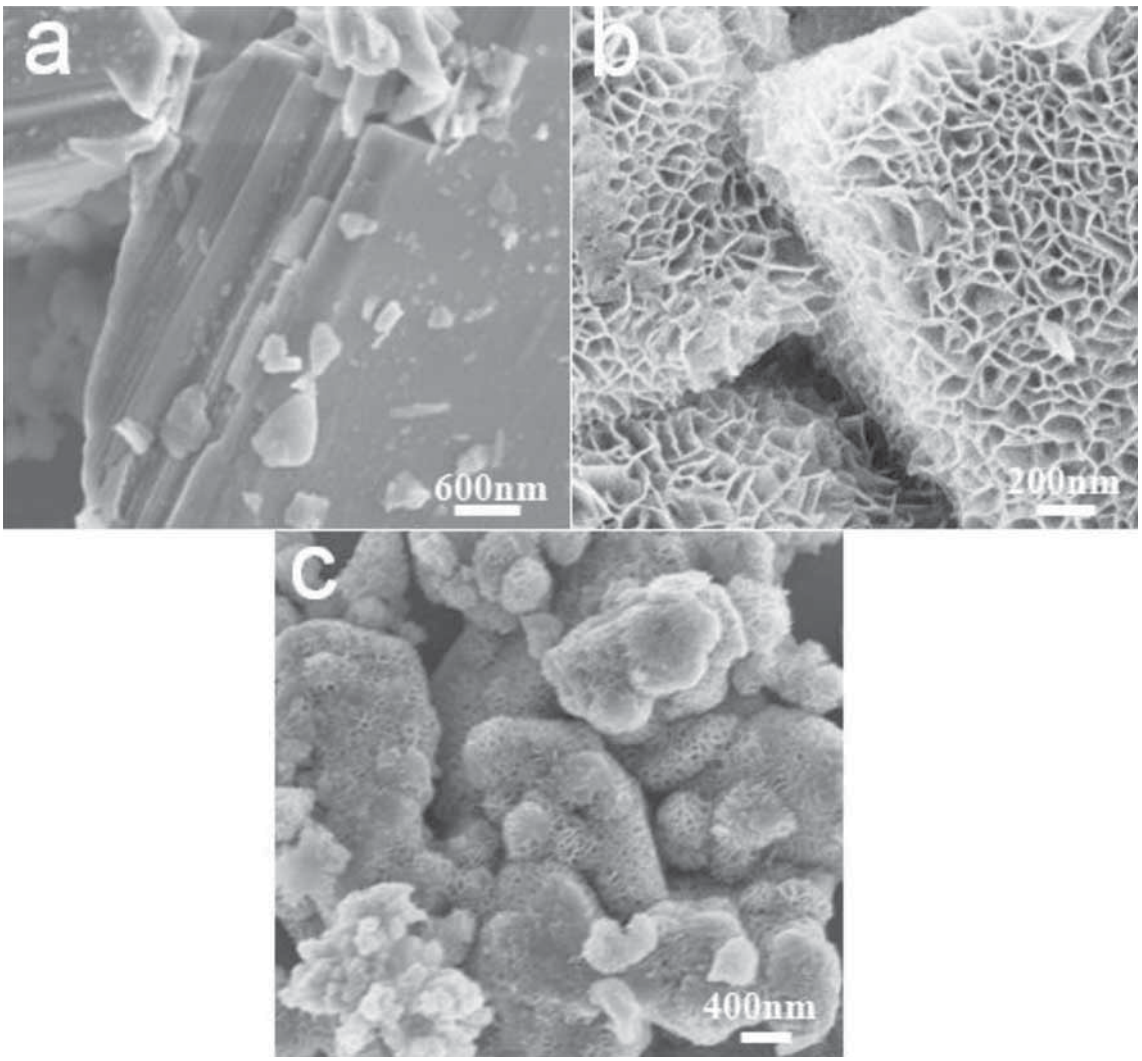

Figure 1. SEM images of the (**a**) as-synthesized $KTiNbO_5$, (**b**) magnetic oxide-pillared $KTiNbO_5$ and (**c**) Au-loaded magnetic oxide-pillared $KTiNbO_5$.

shows the diffraction peak at $2\theta = 12.07°$ can be ascribed to the (110) phase of $MnO_2 \cdot 0.3H_2O$. The XRD pattern of the as-synthesized porous $KTiNbO_5$ exhibited an orthorhombic phase with diffraction peaks of (002) and (102) at 9.026 and 27.52°, respectively. The diffraction peaks at 16.769, 23.94, 28.4, 32.254, 36.9 and 39.5° can be ascribed to the (101), (011), (202), (113), (106) and (203) orthorhombic phases of $KTiNbO_5$. A comparison of the diffraction peaks of (002) at 9.6° of pure $KTiNbO_5$ indicated that the organized layered structure was retained when oxide manganese formed in the interlayers of $KTiNbO_5$, and d-spacing was increased. After Au nanoparticles were loaded in the porous $KTiNbO_5$, a diffraction peak at 38.184° appeared, which is assigned to the (111) phase of Au. Therefore, Au nanoparticle-loaded MnO_2. $0.5H_2O$-pillared porous $KTiNbO_5$ was synthesized through facile ion-exchange, hydrothermal reaction and UV irradiation.

The FTIR spectra of the as-synthesized composites were studied to evaluate the structure of the as-synthesized $KTiNbO_5$-based composites. Supplementary figure S2 shows the pure $KTiNbO_5$ (line a), $MnO_2 \cdot 0.5H_2O$-pillared $KTiNbO_5$ (line b) and Au-loaded porous $KTiNbO_5$ (line c). According to the reported literature [18], the band at 904 cm^{-1} (supplementary figure S2, line a) shows the vibration of Ti=O. The band at 919 cm^{-1} (supplementary figure S2, lines b and c) illustrates the vibration of Nb=O, which indicates the existence of the NiO_6 unit. The band at 503 cm^{-1} corresponds to the vibration of O–Nb–O, and the band at 629 cm^{-1} represents the O–Ti–O vibration (supplementary figure S2, lines a, b and c). The band at 1632 cm^{-1} (supplementary figure S2, lines b and c) corresponds to the vibration of hydroxyl-absorbed physically, and hydroxyl-absorbed chemically was marked at 1423 cm^{-1}; this result is consistent with the FTIR spectra of MnO_2 reported by Chu *et al* [19]. Bands at 3438 (line a) and 3417 cm^{-1} (lines b and c) are attributed to the combined vibrations of H_2O. Similar to the XRD results, the FTIR spectra indicated the presence of $KTiNbO_5$ and Au composites.

Supplementary figure S3 shows the nitrogen adsorption–desorption isotherm for the as-synthesized MnO_2-pillared $KTiNbO_5$. A typical IV hysteresis loop could be classified in the range $p/p_0 = 0.5-1.0$, which indicates that a porous structure composite was obtained [20]. As it has been confirmed by SEM, a type H3 loop in the isotherm is apparently proven for the formation of slit-like pores. From the adsorption branch of isotherm (supplementary figure S3, inset), it can be seen that the plot of BJH (Barrett–Joyner–Halenda) pore size distribution show a broader distribution of pores. As reported by Wang *et al* [21], the as-synthesized metal oxide nanoparticles into the interspaces may produce many pores between perovskite layers, but the micropores are too small to adsorb N_2 molecules (kinetic diameter of 7 A). Thus, the BET surface area of the as-synthesized MnO_2-pillared $KTiNbO_5$ is about 7.1 $m^2\,g^{-1}$. Furthermore, the thermogravimetric (TG) curve of the as-synthesized porous $KTiNbO_5$ (figure 2, line a) and Au-loaded $KTiNbO_5$ composites (figure 2, line b) in the temperature range of 30−700°C was measured. Two composites have similar loss weight. Figure 2 shows that a slight weight loss up to 300°C for both the lines, which was ascribed to the removal of physically and chemically absorbed water. Another weight loss up to 400 and 560°C was caused by the phase transformation from MnO_2 to Mn_2O_3 in both the composites, accompanied by the change in lattice oxygen and bent manganese [22]. There is no extra weight loss up to 700°C.

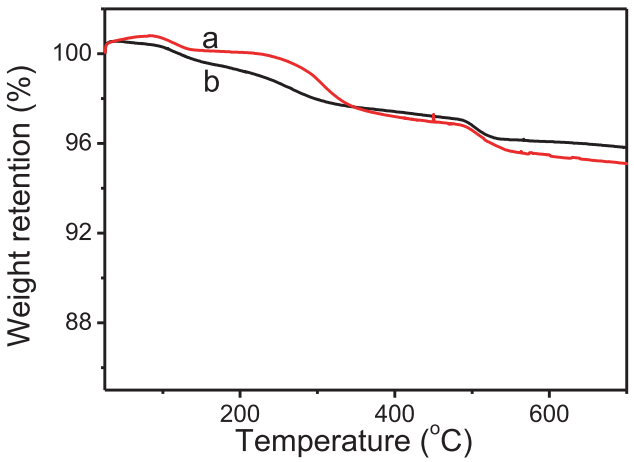

Figure 2. TG curves of the as-synthesized porous $KTiNbO_5$ (line a) and Au-loaded $KTiNbO_5$ composites (line b).

3.2 *Adsorption and photocatalytic degradation of MB*

Considering the porous structure of as-synthesized $MnO_2 \cdot 0.5H_2O$-pillared $KTiNbO_5$ composites, the absorption activity of the as-synthesized composites was investigated by mixing with MB. Different concentrations of MB (10, 20 and 30 mg l^{-1}) were mixed with 175 mg of the as-synthesized $KTiNbO_5$, respectively. Figure 3a, b and c shows that the as-synthesized porous $KTiNbO_5$ has a good absorbed activity to MB and the low concentration of MB could be absorbed quickly. Figure 3a shows that the absorption intensity of MB (10 mg l^{-1}) at 660 nm decreased gradually until it disappeared completely after 30 min; this finding demonstrated well that the existing porous structure of the as-synthesized materials. As a type of photocatalytic material, the use of $KTiNbO_5$ in the degradation of some organic pollutants was widely reported [23–25]. Thus, the photocatalytic activity of the as-synthesized porous $KTiNbO_5$ was also studied. Figure 3d shows that the absorption intensity of MB at 660 nm decreased strongly when mixed with porous $KTiNbO_5$ under mercury light irradiation (500 W), and MB was degraded completely after 20 min. Compared with that of the pure $KTiNbO_5$, the photocatalytic rate of the as-synthesized porous $KTiNbO_5$ was faster. We concluded that the good absorption of the as-synthesized porous $KTiNbO_5$ to MB resulted in sufficient contact with the reactant and catalyst to each other, thereby contributing to the better photocatalytic

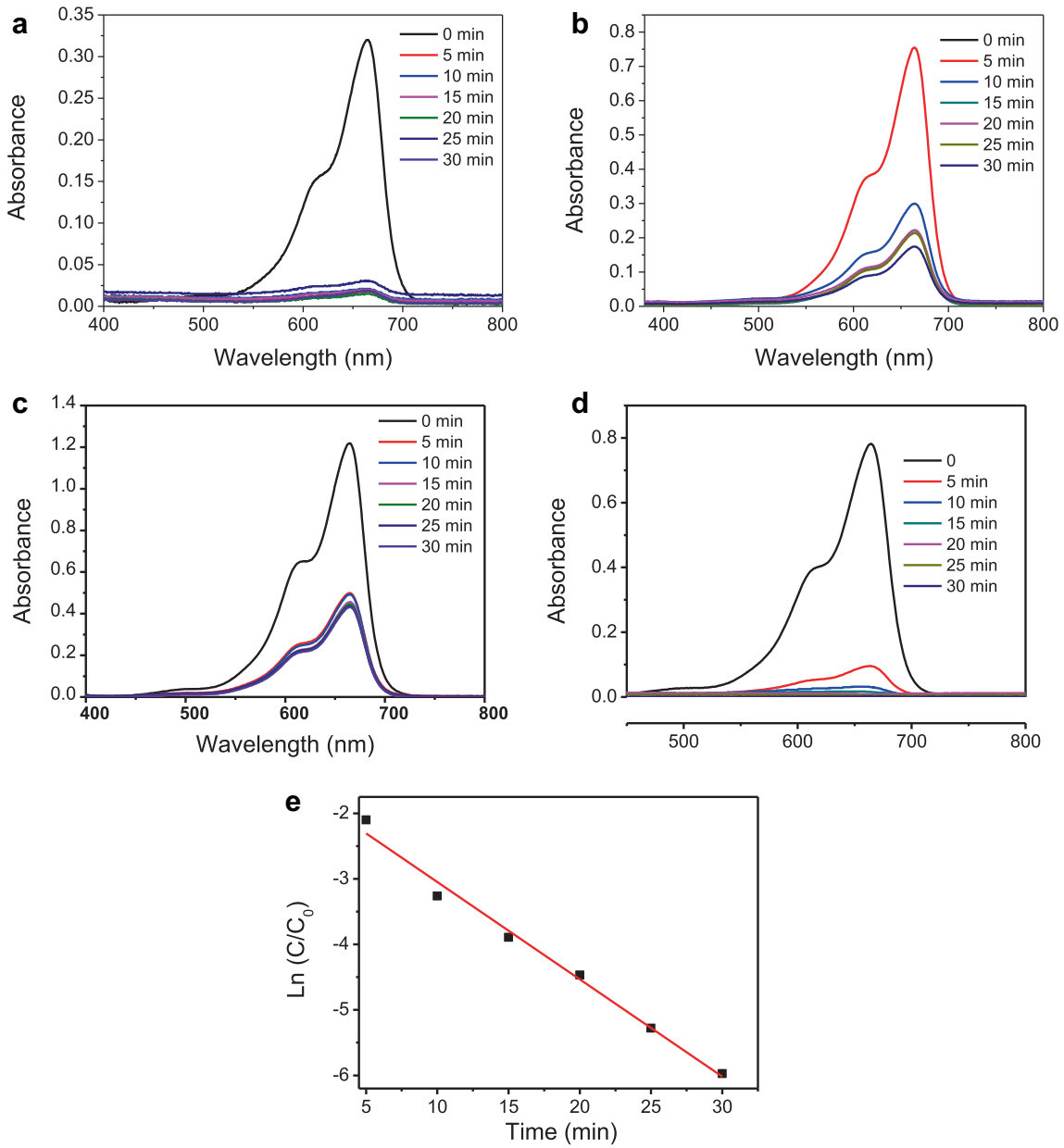

Figure 3. The successive UV–visible absorption spectra of different concentrations of MB after mixing with MnO_2-pillared $KTiNbO_5$ in the absence (**a**, MB, 10 mg l^{-1}; **b**, MB, 20mg l^{-1}; **c**, MB, 30 mg l^{-1}) and presence (**d**, MB, 20 mg l^{-1}) of UV-light irradiation and the relationship (**e**) between $\ln(C/C_0)$ and reaction time (MnO_2-pillared $KTiNbO_5$, 175 mg; MB, 20 mg l^{-1}).

degradation of MB. Thus, a porous $KTiNbO_5$ composite with good absorption and excellent photocatalytic degradation activity for MB was synthesized. Nevertheless, a linear relationship ($R^2 > 0.986$) was established between $\ln(C_t/C_0)$ and reaction time (t) (figure 3e) and the pseudo-first-order kinetics of the reduction reaction was confirmed. Kinetic constant of 0.148 min^{-1} was obtained for the first catalytic cycle. When the obtained k-values were compared with the catalyst of NiO [26] or PW12-APTES@MCF [27], the as-synthesized porous $KTiNbO_5$ has better catalytic properties for degradation of MB.

3.3 *Hydrogenation reducing of p-nitrophenol*

Considering the unique structure of $MnO_2 \cdot 0.5H_2O$ pillared-$KTiNbO_5$ composite, Au nanoparticles were loaded into the composite through reduction of Au ions under UV light irradiation. Then, the MnO_2-pillared $KTiNbO_5$ loaded with Au nanoparticles was used to reduce p-nitrophenol into p-aminophenol. Figure 4a shows that the yellow colour solution (p-nitrophenol) changed into colourless within 20 min after mixing with the as-synthesized composites. Furthermore, the UV spectra (figure 4b) of p-nitrophenol

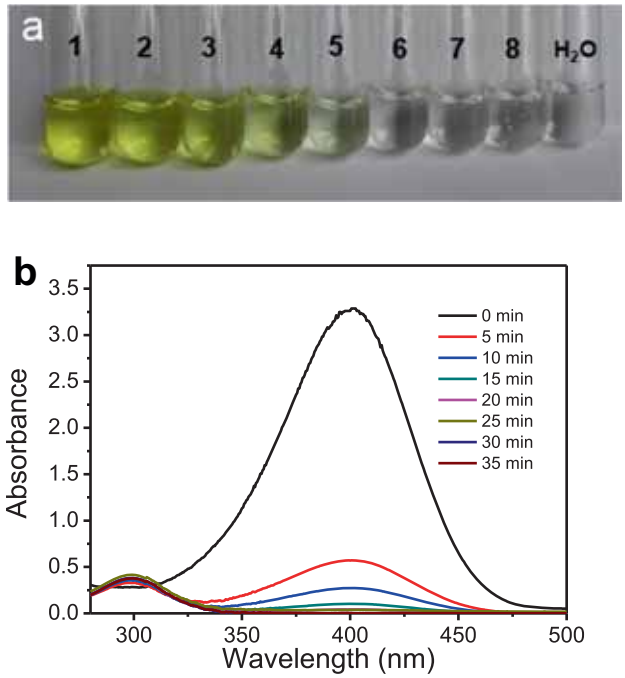

Figure 4. (**a**) The image and (**b**) UV spectra are showing the hydrogenation effect of Au-MnO_2-$KTiNbO_5$ composites on p-nitrophenol (Au-MnO_2-$KTiNbO_5$, 0.25 g; $NaBH_4$, 0.528 mol l^{-1}, 30 ml and p-nitrophenol, 5 mmol l^{-1}, 20 ml).

at 400 nm decreased, whereas the peak at 300 nm (the characteristic peak of p-aminophenol) increased under UV light irradiation. In the end, the peak at 400 nm disappeared completely after 20 min. For comparison, the pure porous $KTiNbO_5$ was used to catalytic reduction of p-nitrophenol under the same conditions. Supplementary figure S4 shows a bad catalytic activity of the as-synthesized porous $KTiNbO_5$ for p-nitrophenol. Thus, we can conclude that Au nanoparticles play an important role in the process of catalytic reducing of p-nitrophenol. Furthermore, recycling activity of the as-prepared Au-MnO_2-$KTiNbO_5$ was evaluated. As it is shown in supplementary figure S5, the catalytic efficiency still yielded favourable results after using the as-synthesized composites for 21 times.

3.4 *Possible catalytic reducing mechanism*

Interestingly, we determined that the time for the first catalytic hydrogenation of p-nitrophenol with the as-synthesized Au-MnO_2-$KTiNbO_5$ was 14 min, and the second recycling time was about 66 min. However, after the third reaction (the third reduction time was about 16 min), the catalytic activity of the as-synthesized composites was enhanced, and the time for the fourth to the 21st reactions was shortened (figure 5). TEM image of the as-prepared Au-loaded MnO_2-pillared $KTiNbO_5$ composites, which was used as a catalyst for the hydrogenation of p-nitrophenol from the

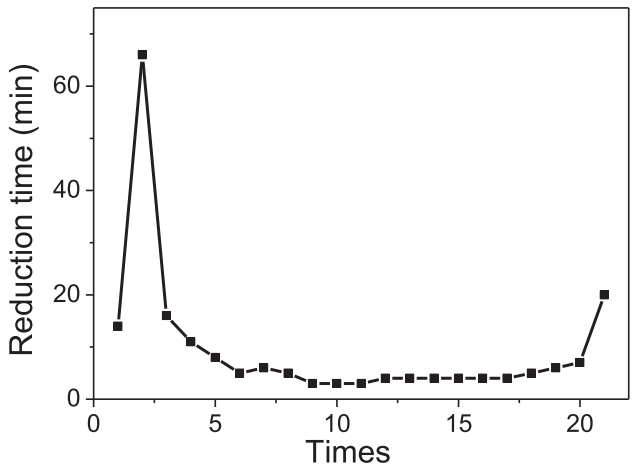

Figure 5. Reaction time of the reducing p-nitrophenol with the as-synthesized composites from the first to 21st times.

first to 21st experiments, was investigated to explore the possible underlying mechanism of the material. The distance between the plates of $KTiNbO_5$ decreased again after it is used in the initial hydrogenation of p-nitrophenol (figure 6a), and the particles could be observed on the surface of the plates (figure 6b, inset). Compared with the sharpening of the as-prepared Au-MnO_2-$KTiNbO_5$ composites, the layered structure of the as-synthesized catalyst diminished completely after 21 times, and the whole pattern became disorder (figure 6b). The image (figure 6b, inset) also shows that the colour of the whole composites changed from black to red (the typical colour of Au nanoparticles) after 21st using. Thus, a possible catalytic mechanism of 'layer-by-layer quilt exposure' mode was proposed. We assume that except for the plates, K^+ on the surface of the nanosheets can be exchanged with Mn ions. Thus, MnO_2 was not only loaded in interlayers, but was also present on the surface of the $KTiNbO_5$ nanosheets. When p-nitrophenol was mixed with the as-synthesized catalyst in the presence of $NaBH_4$, the Au nanoparticles in the pores could relay electrons and react with $NaBH_4$ to generate an active radical. As we know that the MnO_2 particles can strongly catalyse the generation of active radicals, which can affect the sharpening of MnO_2 produced in both the interlayers and on the surface of $KTiNbO_5$ nanosheets. As shown in figure 1, prior to the produced MnO_2 in the interlayers, MnO_2 formed at the surface of the nanosheets reacted with the active radicals, which could further expose the Au nanoparticles loaded into the pores and transferring electrons from $KTiNbO_5$ into p-nitrophenol quickly. However, MnO_2 produced in the interlayers took more attempts to further react with active radicals because of the narrow gaps between $KTiNbO_5$ nanosheets, which resulted in the direct contact of the Au nanoparticles in layers with the nanosheets of $KTiNbO_5$. Thus, a sandwich structure was formed after the fourth recycling process. When the reaction

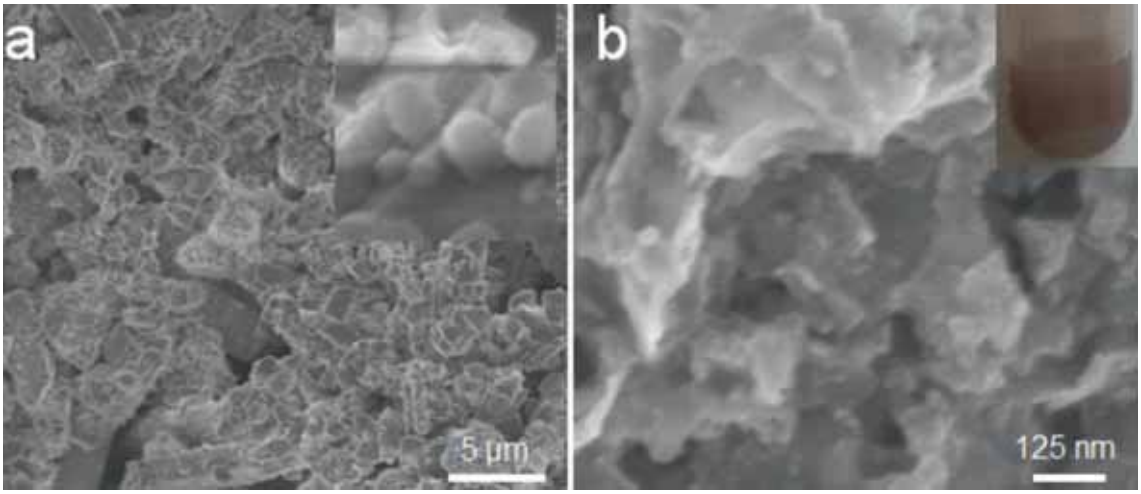

Figure 6. SEM images of the as-synthesized Au-MnO_2-$KTiNbO_5$ composites after it is used to hydrogenate p-nitrophenol for (**a**) the first and (**b**) 21st times, respectively.

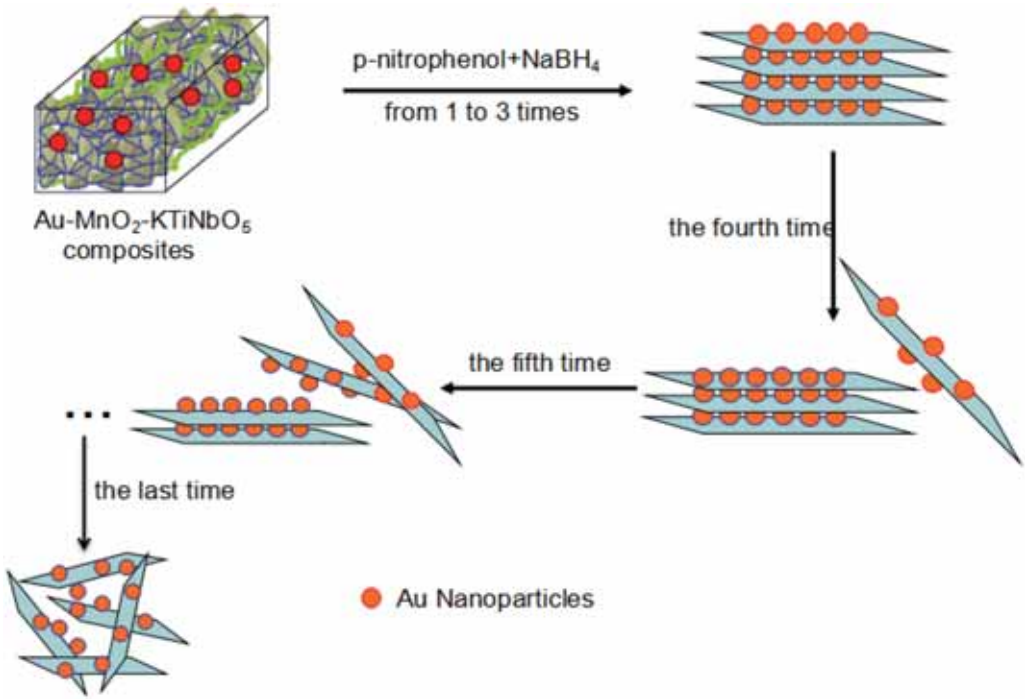

Scheme 2. Schematic illustration of the catalytic mechanism of 'layer-by-layer quilt exposure' mode.

was carried out, the upper nanosheets of $KTiNbO_5$ were revealed and some Au nanoparticles were exposed again, catalytically and effectively hydrogenated p-nitrophenol. With the 'quilts' (nanosheets of $KTiNbO_5$) revealed completely, the disordered structure was finally observed. Thus, we describe the reaction as 'layer-by-layer quilt exposure' mode (scheme 2), but further details and additional evidence were not studied.

4. Conclusion

MnO_2 pillared-layered $KTiNbO_5$ composites with a porous structure were synthesized and used to photocatalytically degrade MB with favourable results. After adsorbing Au^{3+} ions into the MnO_2 pillared-$KTiNbO_5$ composites, the Au nanoparticles were loaded into the porous composites *in situ* under UV light irradiation. No reducing agents

were used to load the Au nanoparticles, which resulted in good catalytic activity of Au-MnO_2-$KTiNbO_5$. Moreover, the as-synthesized composites were used as a catalyst for the hydrogenation of p-nitrophenol. The result shows that the material can be recycled 21 times and still obtained good catalytic activity. Thus, the as-synthesized novel Au-MnO_2-$KTiNbO_5$ composites may be used to develop new methods for constructing $KTiNbO_5$-based catalysts.

Supporting information

XRD data; the FTIR spectra of the as-synthesized $KTiNbO_5$, porous $KTiNbO_5$ and Au-MnO_2-$KTiNbO_5$ composites; N_2 adsorption and desorption isotherms of the MnO_2-pillared $KTiNbO_5$ composites; the recycle effect of the as-synthesized Au-MnO_2-$KTiNbO_5$ composites on the catalytic hydrogenation of p-nitrophenol; and the UV spectra showing the hydrogenation effect of porous $KTiNbO_5$ composites on p-nitrophenol are detailed.

Acknowledgements

This work is supported by the national natural science foundation of China (No. 21505001), the key Young Teacher Project of Anhui University of Science and Technology (QN201313), and the Research Fund for the Doctoral Program of Anhui University of Science and Technology (11109).

References

[1] Bhattacharjee A and Ahmaruzzaman M 2016 *RSC. Adv.* **6** 41348
[2] Feng J, Wang Q, Fan D, Ma L, Jiang D, Xie J *et al* 2016 *Appl. Surf. Sci.* **382** 135
[3] Lin T, Li Z, Song Z, Chen H, Guo L, Fu F *et al* 2016 *Talanta* **148** 62
[4] Zhang W, Zhou Z, Shan X, Xu R, Chen Q, He G *et al* 2016 *New J. Chem.* **40** 4769
[5] Dong Z, Wang T, Zhao J, Fu T, Guo X, Peng L *et al* 2016 *Appl. Catal. A Gen.* **520** 151
[6] Yang P, Xu A D, Xia J, He J, Xing H L, Zhang X M *et al* 2014 *Appl. Catal. A Gen.* **470** 89
[7] Mei L P, Wang R, Song P, Feng J J, Wang Z G, Chen J R *et al* 2016 *New J. Chem.* **40** 2315
[8] Kalarivalappil V, Divya C M, Wunderlich W, Pillai S C, Hinder S J, Nageri M *et al* 2016 *Catal. Lett.* **146** 474
[9] Guo M, He J, Li Y, Ma S and Sun X 2016 *J. Hazard. Mater.* **310** 89
[10] Sygletou M, Tzourmpakis, Petridis C, Konios D, Fotakis C, Kymakis E 2016 *J. Mater. Chem. A* **4** 1020
[11] Wang C, Tang K, Wang D, Liu Z and Wang L 2012 *J. Mater. Chem.* **22** 22929
[12] Liu C, Han R, Ji H, Sun T, Zhao J, Chen N *et al* 2016 *Phys. Chem. Chem. Phys.* **18** 801
[13] Du G H, Yu Y, Chen Q, Wang R H, Zhou W and Peng L M 2003 *Chem. Phys. Lett.* **377** 445
[14] Dias A S, Lima S, Carriazo D, Rives V, Pillinger M and Valente A A 2006 *J. Catal.* **244** 230
[15] Takagaki A, Sugisawa M, Lu D, Kondo J N, Hara M, Domen K *et al* 2003 *J. Am. Chem. Soc.* **125** 5479
[16] Lin H Y and Chang Y S 2014 *Int. J. Hydrog. Energy* **39** 3118
[17] Fan X, Lin B, Liu H, He L, Chen Y and Gao B 2013 *Int. J. Hydrog. Energy* **38** 832
[18] He J, Xu A, Hu L, Wang N, Cai W, Wang B *et al* 2015 *Power Technol.* **270** 154
[19] Chu H Y, Lai Q Y, Wang L, Lu J F and Zhao Y 2010 *Ionics* **16** 233
[20] Kruk M and Jaroniec M 2001 *Chem. Mater.* **13** 3169
[21] Cai W, Lu G, He J and Lan Y 2012 *Ceram. Int.* **38** 3167
[22] Dong Y M, Li K, Jiang P P, Wang G L, Miao H Y and Zhang J J 2014 *RSC Adv.* **4** 39167
[23] Hosogi Y, Kato H and Kudo A 2008 *J. Phys. Chem. C* **112** 17678
[24] Meng L, Zhang X, Tang Y, Su K and Kong J 2015 *Sci. Rep.* **5** 1
[25] Deng R R, Xie X J, Vendrell M, Chang Y T and Liu X G 2011 *J. Am. Chem. Soc.* **133** 20168
[26] Fazaeli R, Aliyan H, Tangestaninejad S and Foroushani S P 2014 *J. Iran Chem. Soc.* **11** 1687
[27] Ranjbar M, Taher M A and Sam A 2015 *J. Mater. Sci. Mater. Electron.* **126** 8029